RESEARCH ARTICLE | OCTOBER 30 2025

A miniature tunnel diode oscillator for condensed matter physics experiments

Ahad Ali Khan ; Kevin Feeny; Brett Laramee ; Charles C. Agosta ; W. A. Coniglio

Rev. Sci. Instrum. 96, 105206 (2025)
https://doi.org/10.1063/5.0284981
CHORUS

Review of Scientific Instruments ARTICLE pubs.aip.org/aip/rsi

A miniature tunnel diode oscillator for condensed matter physics experiments

Cite as: Rev. Sci. Instrum. 96, 105206 (2025); doi: 10.1063/5.0284981
Submitted: 11 June 2025 • Accepted: 4 October 2025 •
Published Online: 30 October 2025

Ahad Ali Khan,[1] Kevin Feeny,[1] Brett Laramee,[1] Charles C. Agosta,[1,a)] and W. A. Coniglio[2,b)]

AFFILIATIONS

[1] Clark University, Worcester, Massachusetts 01451, USA
[2] NHMFL, Tallahassee, Florida 32310, USA

[a)] **Author to whom correspondence should be addressed:** cagosta@clarku.edu
[b)] **Now at:** Garrett Metal Detectors, Garland, TX 75042, United States.

ABSTRACT

We have developed a new design for a small tunnel diode oscillator circuit, which minimizes eddy current pickup in changing magnetic fields, minimizes parasitic reactance for achieving high frequency operation, and is small enough to fit in the confined spaces that are common in high magnetic field dilution refrigerator environments. The new design has been tested up to 1.5 GHz and at temperatures from room temperature down to 25 mK. We have also used the system to take measurements up to 60 T in a pulsed magnetic field. In this manuscript, we analyze the circuit and give guidance for using the circuits and the limits of operation.

I. INTRODUCTION

Tunnel Diode oscillators (TDOs) have been at the heart of many types of condensed matter measurement instrumentation over the past 50 years.[1–5] Particular variations have been optimized for temperature sweeps at constant magnetic fields[6] and others, with variations, such as the proximity oscillator,[7] for very high magnetic fields.[8] We have made improvements to a TDO system for rf penetration depth measurements that is suitable for studying materials at the extremes of low temperatures and high magnetic fields and, in particular, in pulsed magnetic fields. TDO circuits in most high magnetic field systems are confined to small spaces, and this problem is especially true in pulsed magnetic fields resulting in placing the TDO circuit far from the sample measurement coil. The transmission line between the circuit and the coil lowers the operating frequency of the TDO. In addition, in pulsed magnetic fields, the dB/dt of the magnet can induce currents in the circuit that can quench the oscillations. To mitigate these problems, we have developed a TDO oscillator circuit board that is 3×8 mm^2 and can fit into small spaces, such as on the sample rotator in a dilution refrigerator in the bore of the highest field dc or in pulsed magnets at the National High Magnetic Field Laboratory (NHMFL). The small size of the circuit reduces the pickup of rf noise and eddy currents from changing magnetic fields, and its placement allows for higher frequency operation. These characteristics make this new TDO system ideal for the study of novel electronic and magnetic materials with exotic ground states, such as superconductivity and charge density waves, in addition to characterizing electronic structure via Shubnikov–de Haas (SdH) oscillations. In this paper, we will describe the attributes of the new circuit design and parameters for designing an appropriate coil for a particular sample.

The principle of the TDO is simple; a tunnel diode is used to make a tank circuit self resonate at its resonant frequency. A sample under study is placed in the coil of the tank circuit, and the sample excludes the electromagnetic field except for a small penetration depth, resulting in a lower inductance than the empty coil. As the penetration depth of the sample changes, the resonant frequency of the circuit changes, and we measure the change in frequency.

To study new functional materials, it is often useful to use low temperatures and high magnetic fields. These conditions are particularly important for materials with exotic quantum ground states, where energy scales of a few kelvin correspond to tens of tesla, and SdH oscillations can be used to investigate Fermi surfaces. One of the excellent features of the TDO technique is that it is a contactless method, in which the sample is positioned in the center of a coil, eliminating the need for leads directly on the sample. As a

result, there are no problems with contact resistance, very small samples can be studied, and no strains are transferred to the sample by wires, which can broaden phase transitions. Moreover, operating the TDO at tens or hundreds of megahertz allows measurements in a frequency range far away from the common noise sources in dc magnets and especially in pulsed magnetic fields. Using a TDO at low temperatures and high swept or pulsed magnetic fields also requires a minimal amount of copper to prevent eddy current heating, and in pulsed magnetic fields, in particular, there is the added problem of induced voltage in the TDO circuit, which will move the bias voltage on the diode away from its optimum setting. The largest contributor to unwanted induced voltages is the measurement coil itself, and a solution to this contribution, a compensating coil, was proposed over 20 years ago.[3] Minimizing the size of the TDO circuit board also helps reduce induced currents.

A second difficulty encountered over the years is the delicacy of the tunnel diodes, which are heat sensitive, mechanically sensitive, and sensitive to static electricity. Often the diodes are ruined during handling and installation from inadvertent static discharges or while they are being soldered in place. As we will describe below, our new circuits have the diodes fabricated on the circuit board by the manufacturer, avoiding many of the assembly steps where diodes used to be damaged. Once they are in a circuit, they are protected by other circuit elements and rarely fail.

The TDO was first employed in condensed matter physics in 1969,[1] and the seminal description of the circuit was given by Van DeGrift in 1975.[2] We employ a variation of the Van DeGrift circuit shown in Fig. 1 with the following variations. First, we use small coils to increase the filling factor for small samples. Many novel materials can only be grown as single crystals with dimensions much less than a millimeter. In addition, because we often make penetration depth measurements in pulsed magnetic fields, it is important to reduce induced voltages generated in our sample coil. Therefore, we either compensate our coils or keep the coil size small enough, given the dB/dt of the particular magnet, to keep the bias voltage on the tunnel diode within the bias range that produces oscillations, or stable to within 1 mV when we can, for maximum frequency stability. A result of using small coils is that it is not necessary to tap the coil as Van Degrift did, first because the Q of the resonator is low enough to be near the limits of oscillation and second because it would be physically difficult to attach a wire to a selected turn in such a small coil. The other major difference in our setup of the circuit is that we separate the bias network (R_1 and R_2) from the rest of the TDO circuit because it creates a major fraction of the heat in the circuit, instead, placing it higher up in the cryostat to prevent heating the sample area. This is particularly important in a dilution refrigerator, and it is common in a dilution fridge to place the bias network at the level of the 1 K pot. The heat generated by different parts of the circuit is estimated by the design calculator on our website as part of the calculation of the size of the components as specified by Van DeGrift's paper.

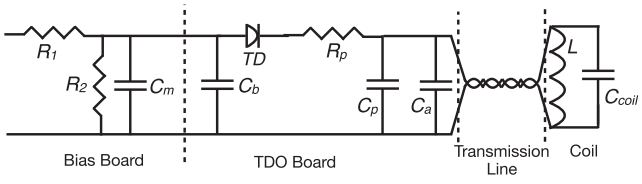

FIG. 1. TDO circuit diagram. The circuit is usually split into three boards: the bias board, the TDO board, and the sample holder, often a piece of 4 × 4 mm sapphire with the measurement coil and the sample inside the coil. C_m softens the termination of the long coax between the bias and TDO boards. Otherwise, that coax length might appear to be an open or short circuit depending on frequency, possibly even acting as a resonant element on the oscillator in the worst case. The transmission line between the coil and the TDO circuit board is sometimes just a twisted wire pair coming directly from the coil a centimeter or two away, but it is best to minimize the length of the twisted pair and switch to coax cable as soon as possible (within a couple mm) to create a well defined ground. Other times, the transmission line might have 3–10 cm of small coax because the TDO board may not fit near the measurement cell.

II. THE CIRCUIT

The layout of the new circuit board is shown in Fig. 2, and as mentioned, a major feature is its size, roughly 3 × 8 mm^2. The size was a compromise. On the one hand, it needs to be as small as possible to prevent dB/dt pickup and to have the ability to place it on rotating platforms in confined spaces, such as in dilution refrigerator mixing chambers in the highest magnetic fields available. On the other hand are the practical considerations, such as soldering chip resistors and capacitors on the board, in addition to finding non-magnetic components in the correct sizes. Besides being non-magnetic, the components should have small temperature coefficients even at millikelvin temperatures. For resistors, nichrome elements are very stable down to low temperatures. In contrast, a typical RuO chip resistor has orders of magnitude resistance increase at low temperatures and makes them great thermometers, but terrible stable circuit elements. For capacitors, we have had the best results with NPO dielectrics. Examples are the PNM series of resistors and the JV series of capacitors both from Vishay. Unfortunately, they all have been difficult to find in stock at distributors in recent years. There is a series of capacitors, Syfer non-magnetic (copper barrier) FlexiCap-terminated ceramic capacitors, that has been in good supply lately.

One of the major innovations of this circuit, mentioned earlier, was to have the bare germanium diodes mounted on the boards by the diode manufacturer, Eclipse Microwave. In this way, we do not have to handle the diodes separately and risk subjecting them to static electricity, nor do they need to be soldered in place. Each board has two diodes in parallel, and each diode has a peak current

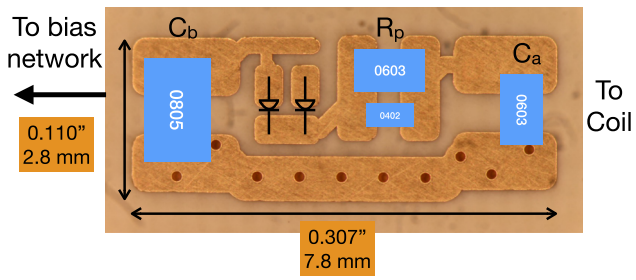

FIG. 2. Bare circuit board showing the position and sizes of the various components.

of nominally 250 or 500 μA. 150 μA diodes will be available in the future. The boards were configured with two small diodes, two large diodes, or one of each. By scratching off the trace that connects one diode to the circuit or repairing the trace with silver epoxy, such as Epo-tek H20E, the diodes can be used separately or in parallel, allowing the circuit to be configured with 250, 500, 750, or 1000 μA as the peak current.

A couple pictures of the circuit board and the measurement coil are shown in Fig. 3. In one case, two circuits and sample coils fit on the rotator built for the dilution refrigerator in the 32 T all superconducting magnet at the NHMFL in Tallahassee, Fl. The part of the probe in the picture is immersed in the mixing chamber. The coils are directly connected to the circuits with a short length of twisted pair formed by the ends of the coil wire. In the other example, the 7.7 mm diameter rotator that is compatible with our 18 mm bore pulsed magnet has space only for the coil on the rotating platform. A 2 cm length of coax connects the coil to the TDO circuit. In this case, the probe is in liquid in a He-3 fridge. The transmission line between the coil and the circuit is critical to the behavior of the oscillating circuit. This behavior is discussed in detail below. The length of the transmission line between the main circuit and bias board can be an issue at high frequencies, and a capacitor at the bias board, C_m, as shown on the circuit diagram in Fig. 1, can help tune the line to avoid a node at the bias board. The transmission line up to room temperature is usually long enough that its actual length does not matter.

In the following sections, we will discuss the behavior of the circuit with coils of different sizes and geometries, focusing on the expected frequency of oscillation and the criteria for oscillation, along with some data for use at low temperatures.

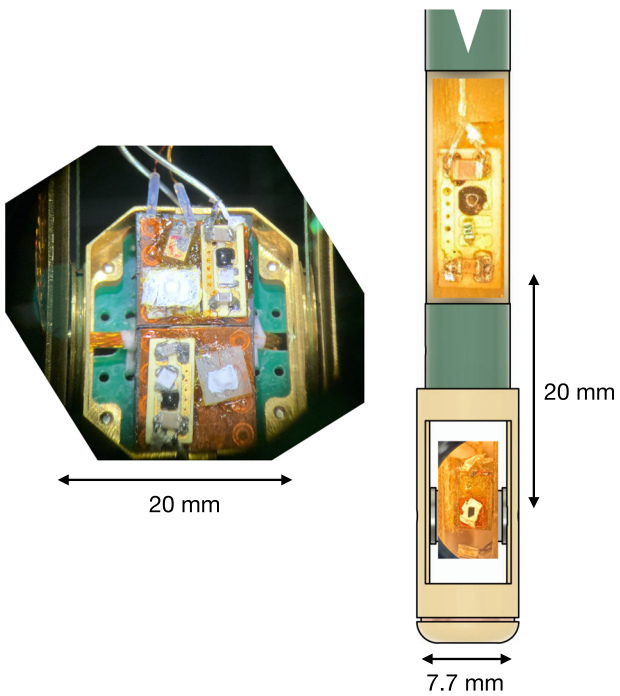

FIG. 3. Examples of the TDO circuit in use. On the left is the rotating platform in the dilution refrigerator used in the 32 T all superconducting magnet at the NHMFL. Two TDO circuits can be seen next to their respective measurement coils with samples. The samples and coils are mostly obscured by Teflon tape. On the right is a diagram of the end of our probe for pulsed fields at Clark University enhanced by two pictures. Here, the circuit and sample are separated by 20 mm and connected by a coax cable (not shown). The sample is visible on the rotator and will be held in place by Teflon tape during the experiment. Both pictures are at the same scale, and in both cases, the bias boards containing the voltage divider are roughly 10 cm higher on the probe.

A. Oscillation criteria

As described by Van Degrift, the TDO oscillates when the tunnel diode is biased into its unstable negative resistance region, where it can transfer power to a tank circuit, forming a driven harmonic oscillator. To facilitate a transfer of power from the diode to the tank circuit, the impedance of the tank circuit at resonance must be larger than the absolute value of the negative resistance of the diode. We first describe the coil selection and the expected frequency of oscillation, and then, based on the properties of the coil and its impedance at resonance, discuss the selection of the tunnel diode.

B. The coil

The first step for designing and using a TDO circuit is winding a suitable coil given the size of the sample and its conductivity. In most of our work, we optimize for sensitivity by maximizing the filling factor of the sample in the coil, which sometimes leads to using a racetrack shaped coil, an example of which is shown in Fig. 4. Many single crystal novel materials are on the order of a millimeter or less in their largest dimension, so coils will be of a similar size. Many samples are also quasi two-dimensional (Q2D) platelets, so only a few turns are necessary to make a coil with height greater than the thickness of the sample. Given these constraints, our coils

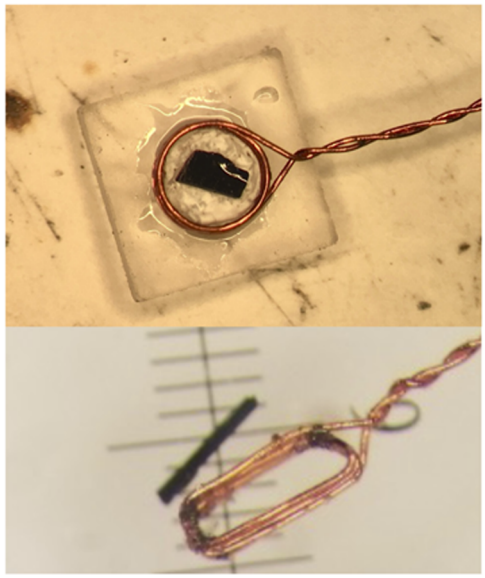

FIG. 4. Two pictures of samples and coils. At the top is a 1.5 mm coil on a 3 × 3 mm sapphire square, and on the bottom is a 0.2 × 0.6 mm coil with a needle-shaped sample next to it. The scale underneath the coil and sample has fine gradations of 0.1 mm.

vary between two and six turns of Nos. 56-45 wire and diameters of 0.2–1.5 mm. If the TDO is going to be used in pulsed magnetic fields, it is also necessary to make sure that coil is compensated even if it is very small. A rule of thumb is to limit the induced voltage due to the magnet pulse to less than 1 mV, although in high dB/dt pulsed fields just staying within the acceptable bias range may be the best you can do. The limit can be found empirically by placing the coil system in a magnet coil and exciting the magnet with an ac source, while measuring the induced voltage from the coil with a lock-in amplifier. The induced voltage on the coil system will be proportional to the dB/dt of the magnet as determined by the amplitude and frequency of the sinusoidal magnet driving current. Given the maximum dB/dt of the pulsed magnet, the coil system can now be adjusted by moving wires around to assure that the coil system will not produce more than 1 mV during a pulse, or at least a voltage small enough not to move the diode bias out of the oscillation region. We note that compensation requires equal turns × area, not equal inductance (which usually goes as turns^2). A single turn of compensation, such as the loop created by soldering to the leads of micro-coax, is often sufficient to compensate the appropriate area, while adding minimal inductance.

The next consideration is the frequency of the measurement. The inductance of the coil, L, the parasitic capacitance of the coil, C_{coil}, the transmission line (twisted pair and coax connecting the coil to the circuit), and the parasitic capacitance of the circuit, C_{p}, along with any added capacitance, C_{a}, will determine the frequency of oscillation. The frequency is important because it determines the rf skin depth in the metallic state of the sample,

$$\delta = 1/\sqrt{\pi\mu_0\sigma f}, \tag{1}$$

where σ is the conductivity of the material, f is the frequency of the rf excitation, and μ_0 is the permeability of free space. Sensitive resistivity measurements require the skin depth to be less than the sample size. Alternatively, if the sample is superconducting, the rf penetration is determined by the London penetration depth, λ_{L}, a length that is frequency independent and usually smaller than δ in the frequency ranges discussed in this publication. The London penetration depth is dependent on the density of Cooper pairs in a superconductor, n_{s}, by the relation, $\lambda_{\text{L}} = \sqrt{m_{\text{e}}/\mu_0 e^2 n_{\text{s}}}$, where m_{e} is the mass of the electron.

We are often interested in measuring resistivity, in particular, to measure Shubnikov–de Haas oscillations. Although many materials of interest have good conductivity and have dimensions on the order of a millimeter, some novel materials do not have great conductivity (at the temperature of interest), or are submillimeter in size, or are inside the tiny sample space in a diamond anvil cell. Using an example of a material with 1/100 the conductivity of copper ($\sigma_{\text{Cu}} = 5.88 \times 10^7$ S/m) and 20 μm in its smallest dimension, the frequency should be above 400 MHz based on Eq. (1) to prevent penetrating the entire sample and losing measurement sensitivity.

C. Frequency

Van DeGrift and Love[9] and Gevorgyan *et al.*[10] treat the frequency of oscillation of a TDO in detail, including second-order effects due to the diode junction capacitance, $C_{\text{d}}(V_{\text{d}})$, and negative resistance of the diode, $R_{\text{n}}(V_{\text{d}})$, both of which are functions of the bias voltage, V_{d}, on the diode. These are important effects for understanding the stability of the oscillator, and as calculated and tested, can change the frequency by 0.1%,[9–11] a much larger change than the desired details in many of our experiments. For our configuration, an estimation of this effect can be calculated from the result found in Gevorgyan *et al.*, reproduced here for a coil that is not tapped (X = 1 in their expression) and has a decent Q, such that R, the resistance of the coil, is $\ll R_{\text{n}}$. In that case, the frequency of the circuit,

$$\omega = \sqrt{\frac{1 + R_{\text{p}}/R_{\text{n}}(V_{\text{d}})}{LC[1 + R_{\text{p}}/R_{\text{n}}(V_{\text{d}}) + C_{\text{d}}(V_{\text{d}})/C]}}, \tag{2}$$

where in this case, $C = C_{\text{p}} + C_{\text{a}} + C_{\text{coil}}$, because there is no transmission line to separate these parallel capacitances. It is important to note that the change in the frequency due to the changing negative resistance is a bigger effect than from the changing diode capacitance. In Sec. II D, we show an example of the variation of the negative resistance and how to measure it. In any case, the expression in Eq. (2) shows the importance of adding capacitance C_{a} to the circuit to minimize the effects of a changing bias voltage, unavoidable in a pulsed field experiment and sometimes a source of noise in dc fields too.

In our case, the coil is small, and we often need a twisted pair, coax, or combination of both to connect the circuit to the coil. In many cases, the transmission line is long enough to be significant, if not dominant in the resonant circuit. A good example of this situation is in a rotating diamond anvil cell, where the coil may be 0.2 mm in diameter but the transmission line 2 or 3 cm long to allow the cell to rotate.[12] For this analysis, we will neglect the second-order effects of the diode and bias voltage and consider the first-order effect of a transmission line with reactive behavior of a similar magnitude of the coil.

Given the small size of the coils, the parasitic reactive elements of the circuit are significant and they are also hard to measure. One can start by isolating just the coil and associated twisted pair tail. With a network analyzer (see Table I), we measured the resonant frequency, inductance, capacitance, and impedance at resonance of the coil and twisted pair. This is done by measuring the impedance at low frequency, where the inductance dominates, at high frequency,

TABLE I. Measurements of the coils and tail (twisted pair leading to the coil) using a network analyzer. The inductance is measured below the resonant frequency, and the capacitance is measured above the resonance. At resonance, the impedance is real. In this table, d_{w} is the diameter of the wire in mm, dia is the diameter of the coil, N is the number of turns, tail is the length of the tail in mm, and L is in nH. TDO_{Res} is the resonant frequency when connected to the TDO, as described below. All capacitances are in pF and frequencies are in MHz.

d_{w}	Dia	N	Tail	L	Z_{Res}	f_{Res}	C	TDO_{Res}
0.0447	1.000	2	3.0	9.5	1500	1996	0.21	1185
0.0447	1.000	3	3.0	18.9	7700	1390	0.45	932
0.0447	1.000	4	2.0	25.0	7100	1320	0.36	687
0.0447	1.000	5	2.5	35.2	9000	1128	0.43	626
0.0447	1.000	6	2.5	59.0	10 500	772	0.74	600

where the capacitance dominates, and at resonance where the imaginary part of the impedance is zero and we can measure the real part exclusively. It is important to emphasize that these measurements include the twisted pair transmission line connecting the coil to the network analyzer.

To help separate all of these effects, we need to estimate the capacitance of just the coil and the twisted pair (or coax) independently. For the coil capacitance, we use the formula for the capacitance of two parallel wires,

$$C_{\text{coil}} = \frac{\ell \pi \varepsilon_0 \varepsilon_r}{\cosh^{-1}(d/2r)}, \tag{3}$$

where ℓ is the circumference of the coil, ε_0 is the permittivity of space, ε_r is the relative permittivity of the dielectric insulation of the wire (adjusted because the electric field of the wire is mostly in air or helium), d is the distance between the centers of the wires in the coil, and r is the radius of the wire. This is the capacitance between the two adjacent turns in the coil, so the total capacitance is the series addition of N-1 turns for the coil. As an example, for a three turn, 0.5 mm in diameter coil wound with No. 50 wire, the capacitance between two turns = 0.2 pF, so C_{coil} = 0.1 pF. This capacitance is much smaller than the other capacitances in the rest of the circuit, so it can often be neglected. We also calculated the inductance of just the coils using a calculation based on current loops suggested by Purcell.[13] The coil is approximated as a set of closed loops, and the calculation first finds the magnetic field produced by each loop numerically over a sufficient volume of space.[14,15] The total magnetic field of the coil over all space can be found by summing the contribution of all of the loops. The inductance, L, is found by integrating the calculated field over all space to find the energy stored in the field, U, and applying the equation,

$$U = \frac{1}{2} L I^2. \tag{4}$$

An example of results for a list of coils is shown in Table II.

The next step is to model the twisted pair as a transmission line and calculate its effect on the resonant frequency. To model the circuit, including the transmission line between the circuit board and the coil, we used a formulation similar to Brisson and Silvera.[16] The impedance of a transmission line terminated by a load, Z_{coil}, is given by

$$Z_{\text{tl}} = \frac{Z_0(Z_{\text{coil}} + jZ_0 \tan \alpha)}{Z_0 + jZ_{\text{coil}} \tan \alpha}, \tag{5}$$

where Z_0 is the impedance of the transmission line, $j = \sqrt{-1}$, $\alpha = \omega \ell / v$, ω is the angular frequency, ℓ is the length of the transmission line, and v is the speed of propagation in the transmission line. In this case, the load, Z_{coil}, is the parallel combination of the coil impedance Z_L and its parasitic capacitance C_{coil}, thus

$$Z_{\text{coil}} = \frac{Z_L Z_{C_{\text{coil}}}}{Z_L + Z_{C_{\text{coil}}}}. \tag{6}$$

To complete the resonant circuit, the capacitance on the circuit board is needed. The added capacitor to the tank circuit, C_a, is in parallel with C_p, the parasitic capacitance of the circuit board. Therefore, the total capacitance from the board, $C = C_a + C_p$. Combining the three equations above results in the following equation:

TABLE II. Numerical calculations for perfectly circular coils. In this table, d_w is the diameter of the wire in mm, dia is the diameter of the coil, N is the number of turns, L is the inductance in nH, and R_L is the resistance calculated with the rf skin depth at the frequency in the last column. The frequency assumes 1 pF and 2 nH of parasitic capacitance and inductance. $Q = \omega L / R_L$.

d_w	Dia	N	L_{coil}	R_L	Q	Freq
0.0447	1.00	2	7.32	0.515	143.4	1606
0.0447	1.00	3	14.82	0.674	167.0	1210
0.0447	1.00	4	24.05	0.812	181.7	977
0.0447	1.00	5	34.82	0.936	192.5	824
0.0447	1.00	6	46.88	1.052	200.5	716
0.0447	1.00	7	59.94	1.162	206.5	637
0.0447	1.00	8	73.72	1.267	210.7	577
0.0447	1.00	9	88.39	1.369	214.2	528
0.0447	1.00	10	103.79	1.467	217.1	488
0.0447	0.50	2	2.94	0.311	128.2	2159
0.0447	0.50	3	5.76	0.421	150.5	1751
0.0447	0.50	4	9.11	0.518	163.3	1477
0.0447	0.50	5	12.89	0.605	171.8	1283
0.0447	0.50	6	17.00	0.686	177.5	1140
0.0447	0.50	7	21.32	0.763	181.1	1031
0.0447	0.50	8	25.76	0.837	183.0	947
0.0447	0.50	9	30.40	0.909	184.5	878
0.0447	0.50	10	35.19	0.978	185.4	820
0.0447	0.30	2	1.47	0.213	109.6	2526
0.0447	0.30	3	2.80	0.298	129.1	2186
0.0447	0.30	4	4.31	0.374	139.7	1929
0.0447	0.30	5	5.97	0.443	146.3	1729
0.0447	0.30	6	7.73	0.508	150.4	1573
0.0447	0.30	7	9.54	0.570	152.4	1450
0.0447	0.30	8	11.37	0.630	153.2	1351
0.0447	0.30	9	13.25	0.688	153.5	1268
0.0447	0.30	10	15.18	0.743	153.6	1197
0.0447	0.20	2	0.84	0.158	92.0	2753
0.0447	0.20	3	1.56	0.227	107.8	2499
0.0447	0.20	4	2.34	0.289	116.2	2287
0.0447	0.20	5	3.18	0.348	121.3	2111
0.0447	0.20	6	4.06	0.403	124.3	1964
0.0447	0.20	7	4.95	0.457	125.6	1844
0.0447	0.20	8	5.84	0.508	125.9	1743
0.0447	0.20	9	6.74	0.557	125.8	1656
0.0447	0.20	10	7.67	0.605	125.6	1579

$$Z_{\text{res}} = \frac{Z_{\text{tl}}}{1 + j\omega C Z_{\text{tl}}} \tag{7}$$

for the whole resonant circuit. We chose to evaluate Eq. (7) with a symbolic equation editor to rationalize it and isolate the imaginary part, which contains over 20 terms. The zeros of the imaginary term are the resonant frequencies of the circuit. An algorithm to find the zeros of this imaginary term can be found on our website. An example of the imaginary value of the impedance showing the resonances is in Fig. 5. The limits of the imaginary part of Eq. (7) at high and low frequencies can be used to find the inductance and capacitance of the transmission line. For example, 4 mm of twisted pair (Z_0 = 65 Ω, $v = 2.0 \times 10^8$ m/s) yielded C = 0.2 pF and L = 17 nH.

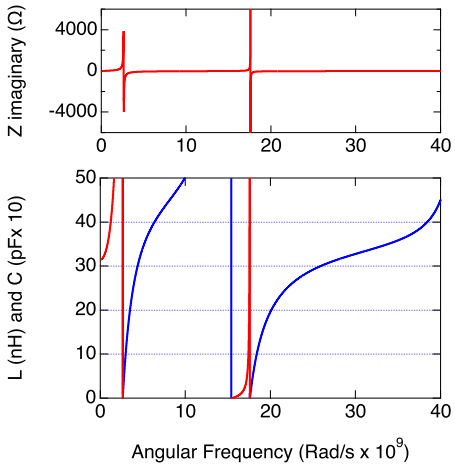

FIG. 5. Top graph showing the imaginary part of the oscillation circuit impedance, including the coil, the transmission line, the parasitic capacitance from the circuit board, and any added capacitance. In this frequency range, there are two resonances. The lower graph shows the inductance and capacitance of the circuit as calculated by setting $L = Z/\omega$ (red) and $C = -1/\omega Z$ (blue), where Z is the result of Eq. (7), the imaginary part of the impedance. The inductance is dominant at low frequencies and the capacitance at high frequencies. In this example, the capacitance is ≃3.2 pF and the inductance of the circuit is ≃31 nH.

Extending the length to 4 cm increased C to 2.3 pf and L to 30 nH. To test this formula for the coil and tail combination, we first look up the inductance for the 1.0 mm diameter, four turn coil from Table II, which is 24.05 nH. Substituting C_c = 0.4 pF, L_c, and ℓ = 2 mm into Eq. (7) yields L = 24.8 nH and f_{Res} = 1378 MHz very close to the measured values from the network analyzer of 25.0 nH, and 1320 MHz respectively.

Two important rules of thumb come from these calculations and measurements. The actual coil capacitance is often negligible as compared to the twisted pair (if it is longer than a centimeter) and will become even more negligible when we consider the circuit board capacitance, C_p and any added capacitance, C_a to the circuit. As for the inductance, comparing similar coils from Tables I and II, N = 4 turns for example, evidently shows the small increase in inductance due to the effect of the twisted pair.

To aid in coil design and test this equation for the actual TDO circuit, we measured the frequency of oscillation of sets of coils spanning 2–5 turns and 0.2–1 mm diameters with 0–10 pf of added capacitance, a sample of which is in Table III. These measurements were done with a 250 μA TDO board. We note that in this dataset we terminated all the coils with ~3 mm of twisted pair, made from the wire in the coil. With these measurements of the resonant frequencies of many small example coils, we were able to identify typical values for the parasitic contributions to the circuit, which can be used for predicting the frequencies of future TDO setups using Eq. (7). For the smallest coils, anything over 2 cm of twisted pair or other transmission line dominates the reactive components of the circuit. Despite this mitigating factor, the dataset allows us to estimate a number of unknown parameters of our TDO circuit. For example, by fitting the change in frequency of oscillation for a four turn, 1 mm coil as a function of changing C_a, the added capacitance

TABLE III. Coils tested with the TDO. In this table, dia is the diameter of the coil in mm, N is the number of turns, C_a is the added capacitance, and f_{Res} is the resonant frequency. All of these measurements were made with No. 45 wire (d_w = 0.044 73 mm).

Dia	N	C_a	f_{Res}	Dia	N	C_a	f_{Res}
1.00	2	0	1185	0.5	2	0	1454
1.00	2	1.0	942	0.5	2	1.0	1373
1.00	2	3.3	709	0.5	2	3.3	838
1.00	2	5.1	609	0.5	2	5.1	752
1.00	2	10.0	268	0.5	2	10.0	xxxx
1.00	3	0	932	0.5	3	0	1141
1.00	3	1.0	742	0.5	3	1.0	921
1.00	3	3.3	541	0.5	3	3.3	659
1.00	3	5.1	482	0.5	3	5.1	555
1.00	3	10.0	338	0.5	3	10.0	413
1.00	5	0	626	0.5	5	0	918
1.00	5	1.0	485	0.5	5	1.0	723
1.00	5	3.3	362	0.5	5	3.3	525
1.00	5	5.1	335	0.5	5	5.1	461
1.00	5	10.0	245	0.5	5	10.0	345

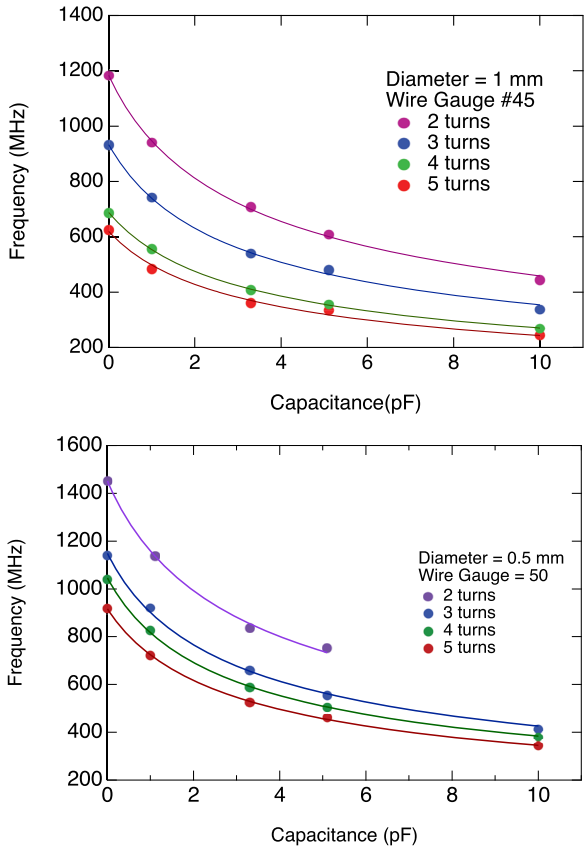

FIG. 6. Graph of frequency vs capacitance for coils of N number of turns connected to a new 250 μA TDO board. The lines are fits to Eq. (8).

in the tank circuit, as in Fig. 6, we can estimate the parasitic capacitance of the circuit. Using the data from the four turn coil and the simple formula,

$$f_{\text{res}} = \frac{1}{2\pi\sqrt{(L)(C + C_{\text{p}})}}, \tag{8}$$

results in $L = 29.3$ nH and $C_{\text{p}} = 1.8$ pF. The network analyzer measurements in Table I show that the coil and tail contributed 25.0 nH and 0.6 pF, respectively. Therefore, the circuit board contributes $1.8 - 0.6 = 1.2$ pF and $29.3 - 25.0 = 4.3$ nH, respectively. These data provide a good model for future coils and setups. The inductance can come from Table I, C_{c}, although probably negligible, from Eq. (3), the coil plus transmission line parameters from Eq. (7), if you are interested in the intermediate results, and then by adding the parasitic values from the TDO board, the final resonant frequency can be calculated, again from Eq. (7).

The following are two examples. For a 1.0 mm, four turn coil using No. 45 wire, $L = 24.05$ nH according to Table II. Assuming a 3 mm tail, 0.4 pF of parasitic coil capacitance [Eq. (3)], a 60 Ω transmission line, and $v = 2.0 \times 10^8$ m/s (as measured with a network analyzer), plus a 1.2 pF of capacitance and a 4.3 nH inductance from the board, then $f_{\text{res}} = 692$ MHz. Connecting the coil to the TDO yielded a resonance of 687 MHz. For a 0.5 mm, three turn coil using No. 50 wire, $L = 5.95$ nH. Assuming a 3 mm tail and the same other conditions of example 1, the calculation result is $f_{\text{res}} = 1194$ MHz, and the measured resonance with the TDO was 1141 MHz. These frequencies are much closer to reality than the simple calculation using the coil inductance and a guess of the parasitic capacitance of 1 pF, which would yield 1010 and 2063 MHz, respectively. We note that both of these examples use no added capacitance on the circuit board, a configuration that we do not suggest for reasons described in Sec. II C.

D. Choosing a diode

To determine the size of the diode (negative resistance) necessary to make a coil oscillate, the quality factor, Q, or more directly the impedance of the oscillator at resonance, Z_{R}, is needed. As mentioned in Sec. I, the circuit will oscillate when the absolute value of the negative resistance of the diode is smaller than the impedance of the coil at resonance. To the extent that the losses in the tank circuit can be represented by the resistance of the coil, R_{c}, the impedance of a tank circuit at resonance is real and equal to

$$Z_{\text{R}} = Q^2 R_{\text{c}} \text{ and } Q = \omega L / R_{\text{c}}, \tag{9}$$

where L is the inductance of the tank circuit and ω is the angular frequency of the circuit. The Q is generally defined as the energy stored in the circuit divided by the energy lost per cycle. Given this definition, the simple formula for Q based on R_{c} is a poor approximation at high frequencies because of radiation losses, which tend to increase as ω^4. Thus, using R_{c} to find Q sets an upper limit on the Q, and a better solution would be to measure the Q directly.

Measuring the Q of small, high frequency coils is difficult. Any method, power reflection using a network analyzer, ringing the circuit with a square wave, or connecting the coil to an oscillating circuit, such as the TDO, and seeing if it oscillates, introduces parasitic elements, which affect the measurement and are hard to quantify. We decided to use multiple ways to measure the Q of a number of coils, including calculating the inductance and Q based on the measurements of the coil's diameter and height and the wire size, included in Table II, and also measuring Z_{R} of some coils with a network analyzer, included in Table I. Possibly the most useful way is to measure the Q *in situ*, a technique we will describe in the next section.

The negative resistance of the tunnel diode can be estimated from the peak current or more accurately by measuring the full I–V curve. Measuring the I–V curve of a tunnel diode is not straightforward, and simply connecting the diode to a source meter, such as a Keithley 2400, does not work because the meter cannot hold the voltage steady in the negative resistance region.[17,18] Making a stiff voltage divider, as we do for the TDO measurements and as shown in Fig. 2, is necessary. More directly, R_2 in the diagram is essentially in parallel with the diode, and if it is smaller in absolute value than the negative resistance of the diode, the voltage source will be stable. In this configuration, we use R_{p} set at 100 Ω as a current shunt to find the current and the voltage difference between the anode and cathode to find the bias voltage. In Fig. 7, the I–V curve is shown for a diode that nominally has a 250 μA peak current. In addition, shown is the reciprocal of the derivative of the I–V curve, $\mathrm{d}I/\mathrm{d}V$, and hence, the negative resistance, which averages ≃ 600 Ω over the useful range of bias voltage. Lower temperatures elevate the peak current a bit, and hence, decrease the absolute value of the negative resistance, allowing the circuit to work with smaller coils and a slightly larger bias range. In some cases, a circuit will only start to oscillate at lower temperatures, where the diode is stronger and the coil resistance is lower, and this effect is somewhat reversed at high magnetic fields due to the magnetoresistance of the coil wire. There is a delicate balance between having enough power to make the circuit oscillate, but not overdriving it to the point where the oscillations become anharmonic. The feedback in the circuit that keeps the oscillations at the resonant frequency is the phase difference between the driving

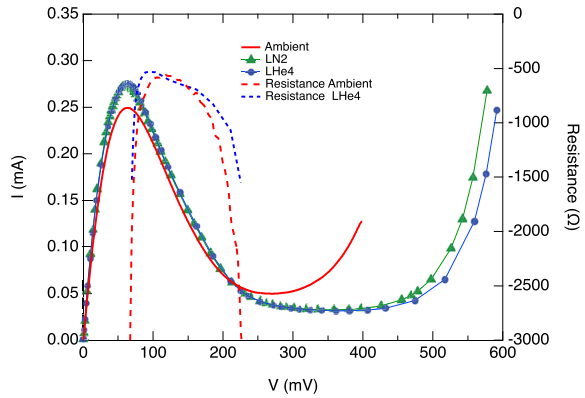

FIG. 7. I–V curves for a nominally 250 μA tunnel diode at room temperature, 77, and 4.2 K. The inverse of the derivative yields the effective resistance of the diode. The negative resistance in the useful region ranges from about an absolute value of 550–800 Ω as the bias voltage changes from 90 to 180 mV. The absolute value of this resistance is compared to the resistance of the resonant circuit at resonance to determine if the circuit will oscillate.

voltage and the oscillations. When there are harmonics in the oscillations, the phase information can become ambiguous. That said, we can see from the Fourier spectrum of our raw oscillations that we are usually overdriving our oscillators. It is difficult not to overdrive them under a cryogenic environment because if they are marginally oscillating at room temperature, they will certainly be overdriven at 4 K. We have run some experiments, where the TDO begins to oscillate at about 40 K, but it is difficult to design and test a circuit that is finely tuned in such a way.

One difficult question to answer is the actual Q of these oscillators *in situ*, but with an accurately measured I–V curve, another estimate of the Q of the circuit can be made. Given the oscillation condition that the absolute value of the negative resistance must be less than the impedance of the resonator (tank circuit plus transmission line) at resonance (Z_{res}), the limits of the oscillation as a function of bias voltage should result in a similar value of the negative resistance on the high and low end of the bias range. This value sets a lower limit on the value of Z_{res}. As an example, we attached a five turn, 1 mm diameter coil to a 500 μA TDO board. The oscillations quenched at a high and low bias voltage that corresponded to the same R_n of 1600 Ω. This result is to be compared to the network analyzer measurement in Table I, where Z_{res} = 7100 Ω. Adjusting $Z_{res} = R_L Q^2$ by the ratio of frequencies, 1320 MHz for the network analyzer measurement, and 600 MHz for the resonant frequency in the TDO circuit due to added capacitance, Z_{res} = 1470 Ω, a similar magnitude to R_n, as expected. These numbers also yield a Q of 34 and an equivalent R_L of 6 Ω. The high value of R_L (see Table II) suggests that most of the dissipation in the circuit is from radiation, not from ohmic losses in the wire.

Detection circuits have been covered in other publications.[3,11,19] For review, in DC fields, we use a superheterodyne receiver with a bandwidth of 2–12 MHz depending on the frequency shift we expect, and the mixed down frequency is measured with a frequency counter. In pulsed magnetic fields, we use the same superheterodyne receiver, but we digitize its output at an acquisition rate of 20–100 MHz for the duration of the magnet pulse (0.1–0.5 s) and analyze the recorded oscillations in software after the experiment is finished.

The absolute sensitivity of these TDO systems is difficult to determine because we measure irregular samples in small, imperfect, hand wound coils. Prior to estimating the sensitivity, it is illuminating to calculate the signal to noise (S/N) ratios of typical effects that we measure. The noise level in the pulsed field data presented in Fig. 10 is about 1000 Hz. In the case of the SdH oscillations, the average amplitude of the oscillations is about 250 kHz, so the S/N ratio is about 125:1. For the superconducting transition, the signal change is about 3 MHz. In that case, the S/N ratio is 3000:1. One way to estimate the absolute sensitivity of this TDO system is to compare recent measurements of the superconducting transition to previous results. The superconducting transition in Fig. 11 is roughly 2 MHz. An estimate of the London penetration depth in organic superconductors is 400 nm.[20,21] The in-plane conductivity of similar samples is roughly 0.1 mΩ cm.[22] Using Formula (1) and the base frequency of the TDO in Fig. 11 of 193 MHz, we can calculate that the rf skin depth is roughly 10 μm. Therefore, the change in penetration depth for the superconducting transition is also 10 μm, given that the London penetration depth is negligible. The frequency change of the TDO is proportional to the penetration depth change for small frequency changes,[21] so we can estimate that the frequency change of 2 MHz linearly corresponded to about a 10 μm change in penetration depth. Given the noise level of about 1000 Hz and a corresponding S/N ratio of 2000, which results in a resolution of about 5 nm for this experiment. As described at the end of Sec. B, we tend to measure the filling factor of the sample, so at the low frequency or high resistance limit, as the penetration depth approaches the size of the sample, the sensitivity will diminish, although magnetic susceptibility changes may still shift the oscillation frequency of the TDO. At the limit of high frequency as the penetration depth becomes very small, the frequency shift will also become smaller as the fractional change of the filling factor of the sample diminishes.

We have included three examples that showcase the excellent signal to noise characteristics of the TDO in DC fields when

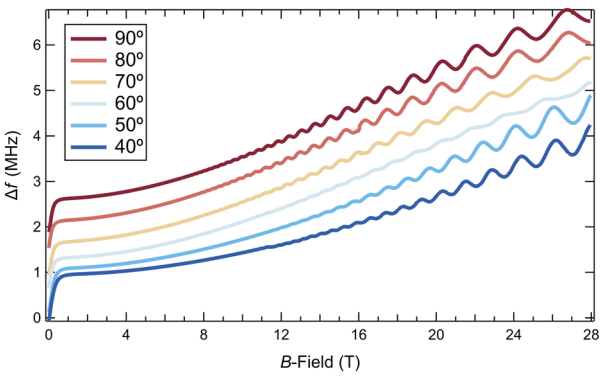

FIG. 8. Shubnikov–de Haas oscillations in the material β″-$(ET)_2[(H_2O)(NH_4)_2Cr(C_2O_4)_3]$•18-Crown-6 measured with the TDO at 50 mK in the all-superconducting magnet at the National High Magnetic Field Laboratory in Tallahassee, FL. The angle is measured between the conducting planes of the sample and the magnetic field, where zero angle is parallel. The TDO base frequency was 453 MHz.

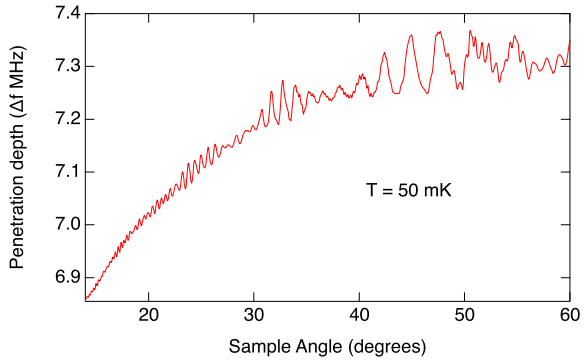

FIG. 9. Angular magnetoresistance oscillations (AMROs) in the material κ-$(ET)_2Cu(NCS)_2$ measured with the TDO oscillating at 472 MHz. It is rare to have signal to noise at the level necessary to see AMRO with a TDO over such a wide angle range with no glitches from wires moving. Here, zero angle corresponds to the magnetic field parallel to the conducting layers. These data were taken at 28 T and 50 mK in the all-superconducting magnet at the National High Magnetic Field Laboratory in Tallahassee, FL.

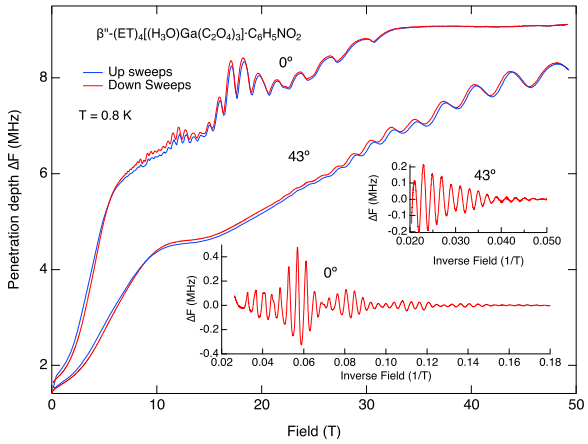

FIG. 10. Superconducting transition and Shubnikov–de Haas oscillations measured with the TDO oscillating at 193 MHz in the pulsed magnetic field at Clark University. The red and blue traces are the up and down traces, respectively. The fact that the traces lie almost exactly on top of each other is evidence of minimal dB/dt pickup or sample heating during the magnetic field pulse. The insets show the SdH oscillations vs inverse field, and the two different angles refer to the direction of the magnetic field with respect to the 2D layers in the material, where zero angle is field perpendicular to the planes.

sweeping the field or the angle and in pulsed fields at a fixed angle. Figure 8 contains field sweeps at fixed angles showing a single frequency of SdH oscillations,[23] and Fig. 9 shows an angle sweep at high magnetic field, both taken in a DC magnet. The small size of the TDO circuit allowed us to mount the board on the rotator directly so that the wires between the sample and the circuit were short and fixed as shown in Fig. 3. In previous experiments, changes in the position of the transmission line between the circuit and sample produced shifts in frequency, degrading the data.

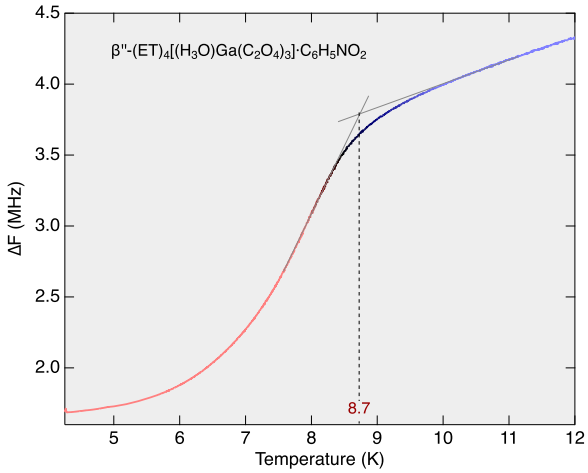

FIG. 11. Superconducting transition measured as a function of temperature. A background should be subtracted from these data, but for robust transitions, such as superconductivity, the raw data are sufficient to easily locate the phase transition.

Figure 10 shows a pulsed field trace using the pulsed magnetic field at Clark University. The large change in frequency up to about 5 T is caused by the superconducting transition. Here, the SdH oscillations are more complex than the ones in Fig. 8, showing a beat structure and an asymmetric shape at high fields. In this setup, the pulse is asymmetrical, the up sweep taking only 11 ms and the down sweep closer to 90 ms. The data are clean with good signal to noise, and most importantly, there is virtually no evidence of dB/dt pickup or sample heating, which would show up as differences between the up and down sweep traces. In all of these data examples, the y-axis is the mixed down frequency of the TDO at the output of a superheterodyne receiver and also in all cases, the TDO is sensitive to the quantum oscillations because of the change in rf penetration as a result of the resistance changing the rf skin depth.[24]

Although it is possible to use this design of the TDO up to room temperature, it is optimized to work at a fixed temperature while sweeping the magnetic field in a dc or pulsed magnet. It would be possible to use the circuit in a different configuration, where the circuit and coil are temperature stabilized (see this reference for example Ref. 6) if temperature sweeps are desired. That said, we have used our system over short temperature ranges to see large scale effects, such as measuring T_c, as seen in Fig. 11. These circuits have been tested and used at the NHMFL in Tallahassee (as seen in Figs. 8 and 9) and Los Alamos and are a regular part of the user programs at both locations.

ACKNOWLEDGMENTS

This research was funded by the NSF Agreement Nos. DMR-1905950 and DMR-2408453. A portion of this work was performed at the National High Magnetic Field Laboratory, which was supported by the National Science Foundation Cooperative Agreement No. DMR-1644779 and the State of Florida.

AUTHOR DECLARATIONS

Conflict of Interest

The authors have no conflicts to disclose.

Author Contributions

Ahad Ali Khan: Conceptualization (supporting); Data curation (equal); Formal analysis (equal); Investigation (equal); Methodology (supporting); Software (supporting); Visualization (equal); Writing – review & editing (supporting). **Kevin Feeny**: Data curation (equal); Formal analysis (supporting); Investigation (equal); Software (equal); Writing – review & editing (supporting). **Brett Laramee**: Data curation (supporting); Formal analysis (equal); Investigation (equal); Visualization (supporting); Writing – review & editing (equal). **Charles C. Agosta**: Conceptualization (lead); Data curation (equal); Formal analysis (equal); Funding acquisition (lead); Methodology (lead); Project administration (lead); Software (supporting); Visualization (equal); Writing – original draft (lead); Writing – review & editing (equal). **W. A. Coniglio**: Conceptualization (lead); Data curation (equal); Formal analysis (lead); Funding acquisition (equal); Investigation (equal); Methodology (equal); Project administration (equal); Writing – review & editing (equal).

DATA AVAILABILITY

Full tables containing all of the data from our measurements of the resonant frequency of coils of different sizes and with various parallel capacitors can be found on our website http://agostalab.clarku.edu/TheTDO.html.

REFERENCES

[1] C. Boghosian, H. Meyer, and J. E. Rives, Phys. Rev. **146**, 110 (1966).
[2] C. T. Van Degrift, Rev. Sci. Instrum. **46**, 599 (1975).
[3] T. Coffey, Z. Bayindir, J. F. DeCarolis, M. Bennett, G. Esper, and C. C. Agosta, Rev. Sci. Instrum. **71**, 4600 (2000).
[4] A. Carrington, I. J. Bonalde, R. Prozorov, R. W. Giannetta, A. M. Kini, J. Schlueter, H. H. Wang, U. Geiser, and J. M. Williams, Phys. Rev. Lett. **83**, 4172 (1999).
[5] H. Kim, M. A. Tanatar, and R. Prozorov, Rev. Sci. Instrum. **89**, 094704 (2018).
[6] R. Giannetta, A. Carrington, and R. Prozorov, J. Low Temp. Phys. **208**, 119 (2022); arXiv:2109.07616.
[7] M. M. Altarawneh, C. H. Mielke, and J. S. Brooks, Rev. Sci. Instrum. **80**, 066104 (2009).
[8] S. E. Sebastian, N. Harrison, M. M. Altarawneh, C. H. Mielke, R. Liang, D. A. Bonn, W. N. Hardy, and G. G. Lonzarich, Proc. Natl. Acad. Sci. U. S. A. **107**, 6175 (2010); arXiv:0910.2359.
[9] C. T. Van Degrift and D. P. Love, Rev. Sci. Instrum. **52**, 712 (1981).
[10] S. G. Gevorgyan, G. D. Movsesyan, A. A. Movsisyan, V. T. Tatoyan, and H. G. Shirinyan, Rev. Sci. Instrum. **69**, 2550 (1998).
[11] W. A. Coniglio, L. E. Winter, C. Rea, K. Cho, and C. C. Agosta, arXiv:1003.5233 [physics.ins-det] (2010).
[12] C. Martin, C. C. Agosta, S. W. Tozer, H. A. Radovan, T. Kinoshota, and M. Tokumoto, J. Low Temp. Phys. **138**, 1025 (2005).
[13] Purcell, Private communication from Edward Purcell, 1987.
[14] W. Smythe, *Static and Dynamic Electricity*, *International Series in Pure and Applied Physics* (McGraw-Hill, New York, 1950), p. 270.
[15] F. Grover, *Inductance Calculations: Working Formulas and Tables*, Dover phoenix ed. (D. Van Nostrand, 2004).
[16] J. G. Brisson and I. F. Silvera, Rev. Sci. Instrum. **57**, 2842 (1986).
[17] L. Wang, J. M. L. Figueiredo, C. N. Ironside, and E. Wasige, IEEE Trans. Electron Devices **58**, 343 (2011).
[18] M. Bao and K. L. Wang, IEEE Trans. Electron Devices **53**, 2564 (2006).
[19] W. A. Coniglio, L. E. Winter, K. Cho, C. C. Agosta, B. Fravel, and L. K. Montgomery, Phys. Rev. B **83**, 224507 (2011).
[20] P. A. Mansky, P. M. Chaikin, and R. C. Haddon, Phys. Rev. Lett. **70**, 1323 (1993).
[21] C. Mielke, J. Singleton, M.-S. Nam, N. Harrison, C. C. Agosta, B. Fravel, and L. K. Montgomery, J. Phys.: Condens. Matter **13**, 8325 (2001).
[22] C. Strack, C. Akinci, V. Pashchenko, B. Wolf, E. Uhrig, W. Assmus, M. Lang, J. Schreuer, L. Wiehl, J. A. Schlueter, J. Wosnitza, D. Schweitzer, J. Müller, and J. Wykhoff, Phys. Rev. B **72**, 054511 (2005).
[23] B. Laramee, R. Ghimire, D. Graf, L. Martin, T. J. Blundell, and C. C. Agosta, Magnetochemistry **9**, 64 (2023).
[24] T. Coffey, C. Martin, C. C. Agosta, T. Kinoshota, and M. Tokumoto, Phys. Rev. B **82**, 212502 (2010).